The periodic table form possible to coincide with a proton distribution

Jianping Mao

201-A-22 Qinye Changzhou, Jiangsu 213016, China
E-mail: mjp00951@163.com

Abstract

The periodic table form seems to coincide with a folding nuclear structure, a distribution of protons (nucleons) nearly the same as Lewis dot structure, which will grow vertical 4 A (representative), 4 B (transition) and 8 C (inner transition) α-clusters bound with valency neutron (excess neutron, ~ $A - 2Z$) to stand a core (1^{st} period) of likely expanding in Co, Ni, Rh and Pd. In a typical fission of $^{235}U+n\rightarrow{}^{137}Ba+{}^{97}Kr+2n$, the mass difference of $^{137}Ba - {}^{97}Kr=40$ is suggested to result from the 16 α-clusters of different length cleft into 9:7 ($\pm$1 A α-cluster, 2 clusters of 5 α) and 2n release from valency neutrons in its scission line; also, the 16 α-clusters cleft into 15:1 implies to point to that α (1 C) and cluster (1 B $\geqslant {}^{12}C$, 1 A $\geqslant {}^{20}Ne$) decay. To cross nuclei, atoms and molecules, this work provides a way that may enable us closer to nature of the periodic table, the periodic law of dominating their behaviors.

Keywords: periodic table, proton distribution, folding nucleus, nuclear core, α-cluster, valency neutron

PACS:

01.30.Kj Handbook, dictionaries, tables, and data compilations

21.10.Dr Binding energies and masses

21.10.Ft Charge distribution

21.10.Gv Nucleon distributions and halo features

21.60.-n Nuclear structure models and methods

21.60.Gx Cluster models

23.35.+g Isomer decay

23.60.+e α decay

23.70.+j Heavy-particle decay

24.75.+I General properties of fission

32.10.-f Properties of atoms

33.15.-e Properties of molecules

Contents:

Introduction

The periodic table with the elements accumulated now is well-known and plays a guide role in physical and chemical fields. Its form, the periodic law, *Z*, the atomic number, is often explained by the electron since it is discovered (1) to establish atomic models (2-4), an atomic periodicity, though about in the same time it has been proven to result from the proton number (5, 6). This seems possible to attribute to that a clear cubic distributions of protons, the atomic number, in a nucleus (7) consisting of protons and neutrons (8) might has not been revealed (9-12), to the best of the author's knowledge. However, it may be a flaw to ignore Moseley's research (5, 6) that the proton number could convey a nuclear periodicity to a certain extent. As the shell model (12), its magic nuclei 2, 8, 20, 28, 50, 82 and 126 is apparently inconsistent with noble nuclei (gases) 2, 10, 18, 36, 54, 86 and 118, while noble nuclei appear to close naturally that could display a cubic *Z* in a tangible proton distributions. It was observed in analysis molecular structure, covering nuclear, atomic and molecular three levels, which is both quite simple and universal.

The observation is starting from a curiosity that whether an atomic mass has an influence upon molecular bond energy or not about in the summer of 1987. Because an element occurs some isotopes and then had no intention of taking their relative mass what want to see nucleons how to distribute in a molecule (atom), every element is represented by its maximal abundant isotope (Table 1) selected from a handbook. The simulation of nucleon distributions of atoms in a molecule is that according to their number of periods and groups. For instance, in $^{12}C^{1}H_4$, the isotopic masses marked in the molecular formula, ^{1}H (99.985%, natural abundance) is simple; ^{12}C (98.89%) is in the 2nd period and group 4A, indicating that its 6 p should be separated into: 2 p in nuclear core and 4 p in nuclear skin, then its 6 n overlap this 6 p frame, that is, $^{12}C_{c\text{-}2+2}{}^{2222}$ (most notes in captions of Table 1, Figs. 1*A*-*C* and 2*A*), which is a tetrahedral distribution to connect 4 ^{1}H atoms, a $^{12}C^{1}H_4$ molecular-nuclear (M-N) structure (Supporting fig. S122), as it is well-known that a methane is a tetrahedral structure. Also, it seems to be straightforward that if alternating single and double bonds of a benzene ring ($^{12,13,14}C_6{}^{1}H_6$, fig. S125), a buckyball ($^{12,13,14}C_{60}$) and diamond ($^{12,13,14}C_n$) are rooted in a tetrahedral nucleus of $^{12,13,14}C$. Here, black and white stones of Go (a Chinese game) were used to stand for protons and neutrons, respectively. It is useful in this early work; without it, it is difficult to simulate a M-N structure, nuclear structure and fission, since a nucleus is a system of numerous nucleons.

In order to test, this proton distribution hypothesis, which could be regarded as nucleon distributions for that neutrons by and large surround protons to fit in a nucleus, is used trying to account for nuclear fission phenomena (13): structures, mass difference and vanishing points of fragments, and emission angle of fission α-particles. Furthermore, it implies that both α and cluster (heavy-particle, mass $A > 4$) decay are similar to fission in principle that only mass ratios are different. Now first is to describe this nucleon distributions which seems to coincide with the periodic law that periods and groups of the periodic table are corresponding to horizontal 7 layers and vertical 16 α-clusters of nuclei, respectively (Figs. 1*A*-*C* and 2*A*). In the 1, 2-3, 4-5 and 6-7 periods/layers or nuclear 0, A, B and C 4 steps, respectively, basic, light, mid and heavy nuclei will be exhibited in nuclear growth (Table 1 and figs. S1-118) to pose different shapes that imply to be folding.

Fig. 1. Nuclear folded and unfolded frames.

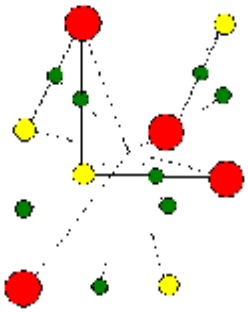

A

	5B				16C	8C		5A	1A		1C	9C					2B		
1B		107			102	94			87		103	95			112			6B	
	111		75		70	62		83	55		71	63		80		108			
		79		41				51	37				48		76				
			47		23			33	19			30		42					
7C	93	61		29				15	11				24		72	104		2C	
15C	101	69						7	3						64	96		10C	
									1										
4A		82	50	32	14	6		27	28		8	16	34	52	84			6A	
8A		86	54	36	18	10	2	45	46		4	12	20	38	56	88		2A	
										1									
6C	92	60						5	9	2					65	97		11C	
14C	100	68		22				13	17	3			25		57	89		3C	
			40		26			31	35	4		21		43					
		74		44				49	53	5			39		77				
	106		78		59	67		81	85	6	58	66		73		109			
4B		110			91	99				7	90	98			105			7B	
	8B				5C	13C		3A	7A		4C	12C				3B			

B

	1A	2A	3B	4B	5B	6B	7B	8B	9B	10B	1B	2B	3A	4A	5A	6A	7A	8A
1	1																	2
2	3	4											5	6	7	8	9	10
3	11	12											13	14	15	16	17	18
4	19	20	21	22	23	24	25	26	27	28	29	30	31	32	33	34	35	36
5	37	38	39	40	41	42	43	44	45	46	47	48	49	50	51	52	53	54
6	55	56	73	74	75	76	77	78			79	80	81	82	83	84	85	86
7	87	88	105	106	107	108	109	110			111	112						

3C	4C	5C	6C	7C	8C	9C	10C	11C	12C	13C	14C	15C	16C	1C	2C
57	58	59	60	61	62	63	64	65	66	67	68	69	70	71	72
89	90	91	92	93	94	95	96	97	98	99	100	101	102	103	104

C

(*A*) Nuclei seem to grow 4 A ($Z \geqslant$ 10, red), 4 B ($Z \geqslant 26$, yellow) and 8 C α-clusters (axes) ($Z \geqslant 70$, green), where are ^{l}p (last proton, added to the prior element, Z - 1) locations of A (representative), B (transition) and C (inner transition) family elements, respectively. (*B*) Growing locations of ^{l}p of the atomic number 1-112. The period is in the middle (uncolored) and the group is in four sides. The groups 1A, 5A pair on A1 axis, 2A, 6A on A2 axis, 3A, 7A on A3 axis and 4A, 8A on A4 axis; it is the same way for the B and C family groups. Four ^{l}p of Z = 27, 28, 45 and 46 in old group 8B (American convention; groups 8-10, modern form), which was revised into groups 8-10B here, are sunk into the 1st period. (*C*) The A (red), B (yellow) and C (green) families correspond to 4 A, 4 B and 8 C α-clusters, respectively. As 8 C α-clusters occupy 16 ^{l}p, the number of C family elements is suggested to increase from 2×14 to 2×16, then group 8B only leave $_{78}$Pt and $_{110}$Ds. The classification of C family is following previous B family that $_{71}$Lu and $_{72}$Hf of groups 1-2C into inner transition is analogous to $_{29}$Cu and $_{30}$Zn of groups 1-2B into transition, though C shell may have right been closed at $_{70}$Yb (Table 1).

Table 1. A periodic distributions of nucleons for the maximal abundant isotopes.

In expression of nucleon distributions, subscript, left and right superscript of the periodic number are the numbers of ^{v}n, ^{p}n and ^{l}p respectively, and skins are axial configurations that 4 A, 4 B and 8 C axes in 7 codes (the Arabic numeral): 1, proton (p); 2, deuteron (d); 3, triton (t); 4, alpha particle (α); 0, neutron (n); 2, di-neutrons (^{d}n); 3, ^{3}He ion. Hyphen (-) is the same as upside. Chemical valency corresponding to axial configuration is listed in the 2nd period. In the 3rd period is grown mass between these nuclei. There will be a fluctuation only if ^{58}Ni (67.88%) and ^{106}Pd (27.33%) in group 10B are listed.

nucleus	nucleon distribution	chemical valency	grown mass	abundance% /half-lief
^{1}H	1^{a-1}			99.9852
^{4}He	1^{a-1010}			100
^{7}Li	$^{2}1^{2}$ 2^{a-100}	1		92.5
^{9}Be	- 2^{a-2010}	2		100
^{11}B	- 2^{a-0222}	3		80.2
^{12}C	- 2^{a-2222}	4		98.89
^{14}N	- 2^{a-4222}	- 3		99.63
^{16}O	- 2^{a-4242}	- 2		99.75
^{19}F	- 2^{a-4443}	- 1		100
^{20}Ne	- 2^{a-4444}	0		90.5
^{23}Na	- $^{8}2^{8}$ 3^{a-100}			100
^{24}Mg	- - 3^{a-1010}		1	78.99
^{27}Al	- - 3^{a-0222}		3	100
^{28}Si	- - 3^{a-2222}		1	92.2
^{31}P	- - 3^{a-4232}		3	100
^{32}S	- - 3^{a-4242}		1	95.0
^{35}Cl	- - 3^{a-4443}		3	75.77
^{40}Ar	- - $_{4}3^{a-4444}$		5	99.59
^{39}K	- - $^{8}3^{8}$ 4^{a-100}			93.3
^{40}Ca	- - - 4^{a-1010}			96.94
^{45}Sc	- - $^{8}{}_{4}3^{8}$ $4^{b-111\underline{2}}$			100
^{48}Ti	- - - 4^{b-2222}			73.7
^{51}V	- - - 4^{b-4232}			99.75
^{52}Cr	- - - 4^{b-4242}			83.79
^{55}Mn	- - - 4^{b-4443}			100
^{56}Fe	- - - 4^{b-4444}			91.7
^{59}Co	$^{4}1^{3}$ - - 4 -			100
^{60}Ni	$^{4}1^{4}$ - - 4 -			26.23
^{63}Cu	- - - 4 - $^{a-100}$			69.1
^{64}Zn	- - - 4 - $^{a-1010}$			48.9
^{69}Ga	- - - $_{4}4$ - $^{a-111\underline{2}}$			60.0
^{74}Ge	- - - $_{4}4$ - $^{a-3232}$			36.4
^{75}As	- - - $_{4}4$ - $^{a-4232}$			100
^{80}Se	- - - $_{8}4$ - $^{a-4242}$			50.0
^{79}Br	- - - $_{4}4$ - $^{a-4443}$			50.69
^{84}Kr	- - - $_{8}4$ - $^{a-4444}$			57.0

^{85}Rb	-	-	-	$^{16}_{8}4^{16}$	5	a-1				72.17
^{88}Sr	-	-	-	-	5	a-1010				82.6
^{89}Y	-	-	$^{8}3^{8}$	-	5	b-111$\underline{2}$	a-0000			100
^{90}Zr	-	-	-	-	5	b-1212	-			51.46
^{93}Nb	-	-	-	-	5	b-4333				100
^{98}Mo	-	-	-	-	5	b-4343	a-0000			23.78
^{99}Tc	-	-	-	-	5	b-4443	-			2.1×10^{5} yr
^{102}Ru	$^{6}1^{4}$	-	-	-	5	b-4444	-			31.64
^{103}Rh	$^{6}1^{5}$	-	-	-	5	-	-			100
^{104}Pd	$^{6}1^{6}$	-	-	-	5	-	-			10.97
^{107}Ag	-	-	-	-	5	-	a-1$\underline{222}$			51.82
^{114}Cd	-	$^{8}_{4}2^{8}$	$^{8}_{4}3^{8}$	-	5	-	a-11$\underline{22}$			28.86
^{115}In	-	-	-	-	5	-	a-0222			95.72
^{120}Sn	-	-	-	-	5	-	a-3333			32.85
^{121}Sb	-	-	-	-	5	-	a-4333			57.25
^{130}Te	-	-	-	-	$_{8}5$	-	a-4343			34.48
^{127}I	-	-	-	-	$_{4}5$	-	a-4443			100
^{132}Xe	-	-	-	-	$_{8}5$	-	a-4444			26.89
^{133}Cs	-	-	-	-	$^{16}_{8}5^{16}$	6		a-1		100
^{138}Ba	-	-	-	-	-	6		a-1122		71.66
^{139}La	-	-	-	-	$^{16}5^{16}$	6$^{\text{c-1010-100}}$	b-0000	a-0000		99.91
^{140}Ce	-	-	-	-	-	6$^{\text{c-1010-1010}}$	-	-		88.48
^{141}Pr	-	-	-	-	-	6$^{\text{c-1010-111}\underline{2}}$	-	-		100
^{142}Nd	-	-	-	-	-	6$^{\text{c-111}\underline{2}\text{-111}\underline{2}}$	-	-		27.11
^{145}Pm	-	-	-	-	-	6$^{\text{c-2121-212}\underline{2}}$	-	-		17.7 yr
^{152}Sm	-	-	-	-	-	6$^{\text{c-3232-3232}}$	-	-		26.7
^{153}Eu	-	-	-	-	-	6$^{\text{c-4232-3232}}$	-	-		52.2
^{158}Gd	-	-	-	-	-	6$^{\text{c-4333-4333}}$	-	-		24.7
^{159}Tb	-	-	-	-	-	6$^{\text{c-4343-4333}}$	-	-		100
^{164}Dy	-	$^{8}2^{8}$	-	-	$^{16}_{8}5^{16}$	6$^{\text{c-4343-4343}}$	-	-		28.2
^{165}Ho	-	-	-	-	-	6$^{\text{c-4443-4343}}$	-	-		100
^{166}Er	-	-	-	-	-	6$^{\text{c-4443-4443}}$	-	-		33.4
^{169}Tm	-	-	-	-	-	6$^{\text{c-4444-4443}}$	b-00$\underline{22}$	-		100
^{174}Yb	-	$^{8}_{4}2^{8}$	-	-	-	6$^{\text{c-4444-4444}}$	-	-		31.84
^{175}Lu	-	-	-	-	-	6	-	b-1$\underline{222}$	-	97.4
^{180}Hf	-	-	-	-	-	6	-	b-2$\underline{222}$	a-$\underline{2222}$	35.1
^{181}Ta	-	-	-	-	-	6	-	b-322$\underline{2}$	-	99.988
^{184}W	-	-	-	-	-	6	-	b-3333	-	30.7
^{187}Re	-	-	-	-	-	$_{2}6$	-	b-4333	-	62.5
^{192}Os	-	-	-	-	-	$_{6}6$	-	b-4343	-	41.0
^{193}Ir	-	-	-	-	-	$_{6}6$	-	b-4443	-	62.6
^{194}Pt	-	-	-	-	-	$_{6}6$	-	b-4444	-	32.9
^{197}Au	-	-	-	-	-	$_{10}6$	-	-	a-1$\underline{222}$	100
^{202}Hg	-	-	-	-	-	$_{16}6$	-	-	a-11$\underline{22}$	29.7
^{205}Tl	-	-	-	-	-	$_{16}6$	-	-	a-223$\underline{2}$	70.5
^{208}Pb	-	-	-	-	-	$_{16}6$	-	-	a-3333	52.4
^{209}Bi	-	-	-	-	-	$_{16}6$	-	-	a-4333	100
^{209}Po	-	-	-	-	-	$_{16}6$	-	-	a-4342	103 yr

^{210}At	-	-	-	-	-	$_{16}6$ - - a-4442		8.3 h
^{222}Rn	$^{6}{}_{6}1^{6}$	-	-	-	-	$_{16}6$ - - a-4444	$^{4}7$	3.82 d
^{223}Fr	-	-	-	-	-	$^{32}{}_{16}6^{32}$	7 b-0000 a-1	22 min
^{226}Ra	-	-	-	-	-	-	7 - a-1010	1602 yr
^{227}Ac	$^{6}1^{6}$	-	-	-	-	-	$7^{c-1010-100}$ - a-0000	21.77 yr
^{232}Th	-	-	-	-	-	-	$7^{c-1122-1122}$ - -	100
^{231}Pa	-	-	-	-	-	-	$7^{c-1122-1112}$ - -	3.3×10^{4} yr
^{238}U	-	-	-	-	-	-	$7^{c-3332-3332}$ - -	99.27
^{237}Np	-	-	-	-	-	-	$7^{c-2223-2222}$ - -	2.1×10^{6} yr
^{244}Pu	-	-	-	-	-	-	$7^{c-3333-3333}$ - -	8.3×10^{7} yr
^{243}Am	-	-	-	-	-	-	$7^{c-4323-3323}$ - -	7950 yr
^{247}Cm	-	-	-	-	-	-	$7^{c-4323-4322}$ b-2222 -	1.6×10^{7} yr
^{247}Bk	-	-	-	-	-	-	$7^{c-4242-4322}$ - -	1.4×10^{3} yr
^{251}Cf	-	-	-	-	-	-	$7^{c-4343-4342}$ - -	898 yr
^{252}Es	-	-	-	-	-	-	$7^{c-4443-4342}$ - -	350 d
^{257}Fm	-	-	-	-	-	-	$7^{c-4443-4442}$ - a-2222	101 d
^{258}Md	-	-	-	-	-	-	$7^{c-4444-4442}$ - -	52 d
^{259}No	-	-	-	-	-	-	$7^{c-4444-4444}$ b-0222 -	58 min
^{260}Lr	-	-	-	-	-	-	7 - b-2222 -	3 min
^{261}Rf	-	-	-	-	-	-	7 - b-3222 -	65 s
^{262}Db	-	-	-	-	-	-	7 - b-2332 -	40 s
^{263}Sg	-	-	-	-	-	-	7 - b-2333 -	0.9 s
^{270}Bh	-	-	-	-	-	-	$_{6}7$ - b-4323 -	61 s
^{277}Hs	-	-	-	-	-	-	$_{16}7$ - b-4342 a-0000	
^{278}Mt	-	-	-	-	-	-	$_{16}7$ - b-4442 -	7.6 s
^{281}Ds	-	-	-	-	-	-	$_{16}7$ - b-4444 a-2000	11 s
^{281}Rg	-	-	-	-	-	-	$_{16}7$ - - a-2000	26 s
^{285}Cn	-	-	-	-	-	-	$_{16}7$ - - a-3222	29 s
^{287}113	-	-	-	-	-	-	$_{16}7$ - - a-3332	
^{288}114	-	-	-	-	-	-	$_{16}7$ - - a-3333	
^{289}115	-	-	-	-	-	-	$_{16}7$ - - a-4333	
^{290}116	-	-	-	-	-	-	$_{16}7$ - - a-4343	
^{291}117	-	-	-	-	-	-	$_{16}7$ - - a-4443	
^{292}118	$^{6}1^{6}$	$_{4}2^{a-4444}$	$_{4}3^{a-4444}$	$_{8}4^{b-4444\ a-4444}$	$_{8}5^{b-4444\ a-4444}$	$_{16}6^{c-4444-4444\ b-4444\ a-4444}$	$_{16}7^{c-4444-4444\ b-4444\ a-4444}$	

Nuclear 4 steps and 16 *α*-clusters

The 1st period: nuclear core. Folding nuclei appear to be woven of 7 kind of particles: ^{1,2,3}H, ^{3,4}He, valency neutron and di-neutrons (unclear who termed), according to the number of periods and groups, which can be separated into core, middle and skin three parts, core+middle = ^{m}c ($Z \geqslant 11$); skin mass, ^{m}s, its particle structures and distributions is called axial configuration in ground state. Generally, ^{m}c is a noble nucleus and core is a ^{4}He of the closed 1st period in a range Z = 3-26, for it will expand in Z = 27, where Z = 21, 27 and 57 are three key points in proton distributions, implying to differ from prevailing electron distributions (configurations). On the other hand, in nuclear growth a nucleon behavior seems to loom up a tetrahedral shape having some "nucleon valency" (~ 4) to bind other nucleons or basic nuclei (Fig. 2*A*) with an explicit direction, suggesting that a molecular bond may result essentially from this character (Fig. 2*B*).

Figures. 2*A-B* also imply that a nucleus and a molecule able to be a three dimensional structure depend largely on that an α-particle is tetrahedral, a most concise solid structure in nature.

Fig. 2. An images of ^{208}Pb (unfolded) and $^{1}H_2{}^{16}O$.

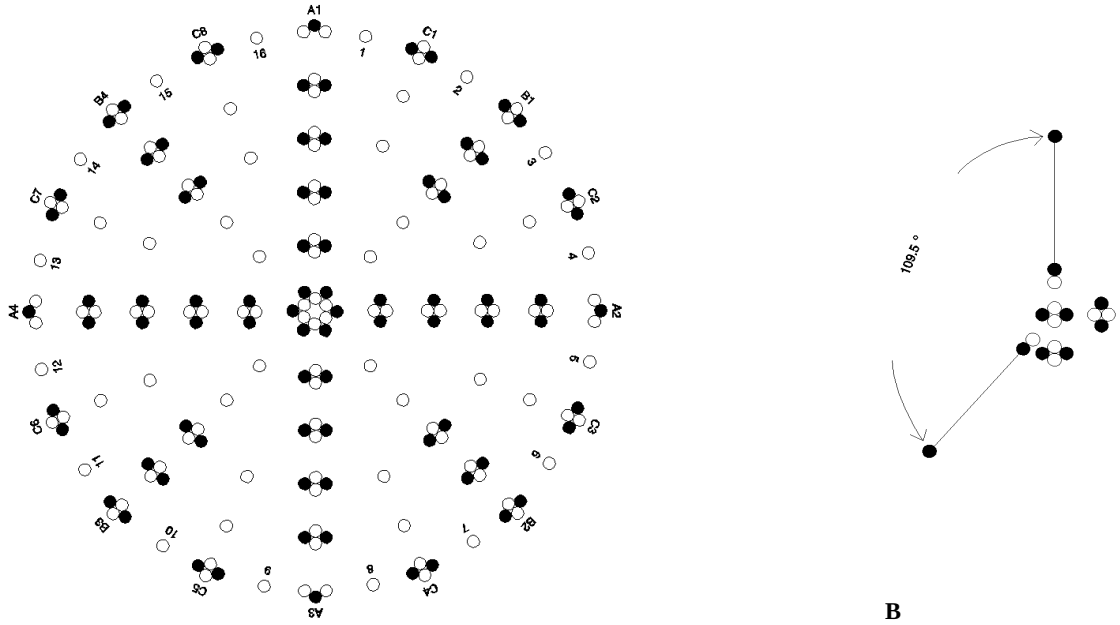

A **B**

(*A*) Closed and open circles are protons and neutrons, respectively. In $^{208}_{82+86+40}Pb_{c\text{-}6+6,v\text{-}40}{}^{c\text{-}4444\text{-}4444,b\text{-}4444,a\text{-}3333}$, right superscript is axial configuration, subscript c-6+6 is core (n+p), v-40 is ^{v}n number and 82+86+40 is Z+^{p}n+^{v}n three frames (shells), where ^{p}n is pair neutron accompanying proton to form ^{2,3}H and ^{3,4}He, and ^{v}n is valency neutron (single open circles) to fill gaps between axes and shells. In order to describe fission, a nuclear coordinate was introduced that the serial numbers of axes and layers are after A, B and C letters; for valency neutron is N and it is clockwise rotating from A1 axis to the origin point: 1→4, 1→8 and 1→16 in A, B and C steps, respectively. This figure suggests that in 1-1/4-8 fission (from N1-6 through 1/4 core to N8-6), 1-8 and 8-1 sectors generally are light (A_L) and heavy (A_H) fragments, respectively (21-23), some of 6 ^{v}n (N1-6, 1-4, 1-2 and N8-6, 4-4, 2-2) are become unbound neutrons (24, 25) in the scission line, and angular distributions of α-particle (26, 27) are 90 - 22.5° for A_L and 90+22.5° for A_H coming from C1-6 or C4-6. (*B*) In the center of $^{1}H_2{}^{16}O$ is a $^{16}O_{c\text{-}2+2}{}^{4242}$ and the farthest are 2 ^{1}H, suggesting that its chemical valency and their angle are rooted in 2 d on the nuclear skin. If the 2 d of $^{16}O^{4242}$ (99.756%) were replaced by 1 or 2 t, it is $^{17}O^{4342}$ (0.039%) or $^{18}O^{4343}$ (0.205%).

The 2-3 periods: Lewis dot structure of nuclear skin. In F_2, O_2 and N_2 molecules, a single, a double and a triple bond coincided with a pair of t in two nuclear skins of $(^{19}F^{4443})_2$, two pairs of d in $(^{16}O^{4242})_2$ and three pairs of d in $(^{14}N^{4222})_2$ suggest that molecular different shapes may be rooted in axial configurations (see also figs. S119-124: $^{23}Na^{35}Cl$, $^{9}Be^{35}Cl_2$, $^{11}B^{19}F_3$, $^{12}C^{1}H_4$, $^{14}N_2$ and $^{16}O_3$, respectively). In the 2nd layer, nuclei start to grow up to 4 α-particles (8 elements) standing on 4 nucleons of a basal tetrahedral α-particle. In $^{7}Li_{c\text{-}2+2}{}^{100}$, axial configuration is a-100 that its 1 ^{1}p with 2 ^{p}n are dispersed on 3 axes of 4 hole axes, thus its skin has merely a proton in that molecular structure is reflected 1 of chemical valency. Generally, the number is equal between chemical main valency and ^{1,2,3}H (p, d and t) at top of nuclear 4 A axes (Table 1), which is nearly the same as Lewis dot structure (3) that an α-particle corresponds to a lone pair of electrons. For example, in ^{16}O, 2 dots and 2 lone pairs of electrons will identify with skin 2 d and 2 α of $^{16}O_{c\text{-}2+2}{}^{4242}$; if 2 ^{1}H atoms descended on the 2 d extended lines, geometrical angle being 109.5° , it is a M-N structure of $^{1}H_2{}^{16}O$ (Fig. 2*B*). At near the 3rd layer end, nuclei begin to grow valency neutrons that first clearly to emerge 4 ^{v}n will be in $^{40}Ar_{v\text{-}4}$ in stable nuclei (~ 300), where the 4 ^{v}n position is to grow out 4 B α-clusters of next step.

The 4-5 periods: nuclear expansible core. Along with nuclear growing to the 4th layer, nuclear skin area will increase enough to hold another 4 B α-clusters (transition metals) in between 4 A α-clusters; further, in order to support increasing mass its core will be intensified in old group 8B. In

terms of electron distributions, proton distribution of $_{21}$Sc is 2 ^{l}p of $_{19}$K and $_{20}$Ca to float on 2 A axes, only the ^{l}p of $_{21}$Sc fit on B axis, but it is not very appropriate from nucleon arrangements of subsequent elements to speculate; i.e., the 3 ^{l}p of $_{19}$K, $_{20}$Ca and $_{21}$Sc should simultaneously glide upon B axes. However, it is hardly possible that protons like electrons is a probability distribution. In comparison, a pair distributions of electrons and protons are $_{21}$Sc:[e-(18)ds^2/p-(18)d^3] (in proton distributions, A = s+p that in the range Z = 3-26, basal 2 p and 2 n which 4 A axes stand on have not been distinguished, B = d and C = f, respectively). Thus, from $_{19}$K to $_{26}$Fe in a total of 8 ^{l}p is piled on 4 B axes. The 2 ^{l}p of $_{27}$Co and $_{28}$Ni begin to sink into the core (Fig. 1*B*). The 2 ^{l}p of $_{29}$Cu and $_{30}$Zn will slip back upon A axes, though they are B family elements, then until to $_{36}$Kr, the 8 ^{l}p are piled on 4 A axes. The 5th layer is the same as the 4th layer, and, the 2 ^{l}p of $_{45}$Rh and $_{46}$Pd in groups 9-10B (Fig. 1*C* and figs. S45-46) have also been sunk into the core, which may be finished that a total of 6 ^{l}p (Z = 1, 2, 27, 28, 45 and 46) with 6 n are to form an innermost close-packed core (Fig. 2*A*).

Originally, here it also felt puzzling that where the ^{l}p of $_{27}$Co should put on. Going through a period of time fiddling with its disorderly nucleon distribution, it seems to indicate that the ^{l}p of $_{27}$Co to put on the center is an optimal option due to ^{56}Fe skin closure, i.e., ^{56}Fe$_{c\text{-}2+2}{}^{4444}$ (91.7%) → ^{59}Co$_{c\text{-}4+3}{}^{4444}$ (100%) (figs. S26-27), $_{27}$Co:[e-(18)d^{7}s^2/p-(19)d^8]. First, it can explain a problem that why exist old group Fe-Co-Ni 8B in the periodic table. Second, this performance will enable a nucleus to possess a definite hub, a Coulomb repulsion center, otherwise its shape can not be opened up, however, like a tiny liquid drop (11). Corresponding to this is in that a chart (14), per nucleon binding energy ~ 8.7 MeV is maximal, as nuclear mass increase to A ~ 60, i.e. Fe-Co-Ni region, which would imply that though at Fe-Co-Ni region the nuclear core has been intensified immediately, a sharp change of nucleon distributions, this curve remains to fall. In addition, ferromagnetic only occurs in Fe, Co and Ni at room temperature which possibly has a link to the nuclear core expansion, i.e. a nuclear structure and vibratory pattern of Fe, Co and Ni. However, the nuclear expansible core in nuclear growth show to be rather suitable, such as c-2+2 in ^{16}O, ^{40}Ca, c-4+4 in ^{60}Ni, ^{88}Sr and c-6+6 in ^{120}Sn, ^{208}Pb these magic nuclei (Table 1).

The 6-7 periods: folding nucleus. One of extraordinary feature in the periodic table is old group 8B existence, implying that nuclei contain a expansible core, the other is the number of inner transition metals, from where a particular place, $_{57}$La:[e-(54)ds^2/p-(54)f^3], start to grow out between 4 A and 4 B α-clusters, implying that nuclei are folding. The extrapolation is that, if C family ^{l}p were fitting on 6 faces or 12 sides of Fig. 1*A*, it needs 12 ^{l}p or 24 ^{l}p, what is both impractical. Therefore, it should averagely vacate 4 sides in the 12 sides that only occupy 8 sides to grow 8 C α-clusters. On the other hand, whether C family contains 14 elements? If so, while assume that α is one of particles to construct a nucleus, as such an odd number of 7 α will be asymmetric in a nuclear shape (coordinate). So far, it is thought that nuclear shapes might have not been so easy to recognize, whereas in here are tangible that nuclear shapes almost are tetrahedral in A step (^{12}C, ^{28}Si) and cubic in B step (^{74}Ge, ^{120}Sn), but in C step (^{208}Pb), the shape would be kept in a phase that between cubic and flat, which may result from a nuclear vibratory pattern that only allows to occur 8 C α-clusters. In fact, this nuclear pattern first is two dimensional using Go game stones to put on the floor (see also figs. S1-125), whereas it is so coincidental that when it is folded into three dimensional, such as ^{12}C, ^{74}Ge and ^{208}Pb (Fig. 2*A*). However, from the number of inner transition metals being 16 or 14, not other numbers, and valency neutron number (see later), it strongly suggests that a nuclear shape is folding; further, the extrapolation of C family 8 α-particles appears helpful to explain angle distribution of fission α-particle (see later).

Vertical 16 α-clusters. As in Table 1, configurations of nuclear vertical 16 α-clusters show to correspond to the groups that is almost the same in a big group, regardless of group A, B and C. For example, in big group 7 (7A, 7B, 13-14C), axial configuration 4443 is always found in ^{19}F, ^{35}Cl, ^{79}Br, ^{127}I of 7A, ^{55}Mn, ^{99}Tc, ^{193}Ir of 7B and ^{165}Ho$^{c\text{-}4443\text{-}4343}$, ^{166}Er$^{c\text{-}4443\text{-}4443}$ of 13-14C. In big group 3, a di-neutrons may often serve as a proton in skins of mid-heavy nuclei; e.g., ^{45}Sc$^{b\text{-}111\underline{2}}$ and ^{89}Y$^{b\text{-}111\underline{2}}$ in 3B, each of them has 3 ^{l}p to stay on 3 axes of 4 B axes, then a ^{d}n will substitute for a proton to occupy a surplus axis, thus, the 4 particles (3^{l}p+1^{d}n) are formed a stable b-tetrahedron out of their ^{m}c, i.e., ^{40}Ar+b-111$\underline{2}$ (^{45}Sc, 100%) and ^{84}Kr+b-111$\underline{2}$ (^{89}Y, 100%), similar to a b-tetrahedron of ^{40}Ar+b-2222 (^{48}Ti, 73.7%) that is different from an a-tetrahedron of such as

^{20}Ne+a-2222 (^{28}Si) (Table 1). In 3A occurs ^{69}Ga$^{\text{a-1111}}$ and 5-6C occur ^{141}Pr$^{\text{a-1010 1111}}$, ^{142}Nd$^{\text{a-1111 1111}}$. In stable nuclei, ^{45}Sc is likely emerging di-neutrons for the first time, which seems a unique structure. In group 1A, a ^{7}Li (92.5%) may prefer a-100 to a-3 (a single triton, alternative) in its skin, including below ^{23}Na^{100} (100%) and ^{39}K^{100} (93.3%), because skin particle masses will smoothly increase from 1 to 4 along with sweeping big groups from 1 (1A, 1B, 1C) to 8 (8A, 8-10B, 15-16C). In other words, nuclear skin may be thicker and thicker from left to right in the periodic table.

Evidently, there is a correspondence between the periodicity of atoms and nuclei that a nuclear axial configuration is repeated in every layer, such as the a-4443 in ^{19}F (100%), ^{35}Cl (75.77%), ^{79}Br (50.69%) and ^{127}I (100%) in group 7A that all of their chemical main valency is − 1. Perhaps, the different physical and chemical properties of A, B and C three family elements are principal rooting in that A long, B mid and C short α-clusters extend a different depths in nuclei (Fig. 2*A*). Such as lanthanide contraction, it may be relevant to C family 16 ^{l}p trapped in 8 C axes where is low lying between 4 A and 4 B axes, implying that nuclear radii (15) might have a link to atomic radii (16). For example, in ^{23}Na^{35}Cl M-N structure (fig. S119), thin a-100 in ^{23}Na may be looser to the ^{m}c than thick a-4443 in ^{35}Cl, somewhat similar to that nucleon halo, if involved nuclear force; i.e., the interstice between the ^{m}c and ^{m}s in ^{20}Ne+a-100 (^{23}Na) is larger than in ^{20}Ne+a-4443 (^{35}Cl), a factor possible influence on their atomic radii (0.15 and 0.09 nm, respectively). However, it seems reasonable to conclude that the short 2-3, long 4-5 and very long 6-7 periods are to originate from nuclear 4 (A), 4+4 (A+B) and 4+4+8 (A+B+C) α-clusters standing on the expanding core (the very short 1 period), respectively. The vertical 16 α-clusters in Fig. 2*A* show to be bound with valency neutrons that are excess neutrons in nuclei in all probability.

Composition of beta stable line

Stable nuclei. A distinction between electron and proton distributions is proton distributions accompanied with neutrons. Generally in a nucleus neutrons exceed protons in number, as the slope of beta stable line (neutron-proton ratios) plotting in a chart (17), suggesting to derive from

$$A = Z + {}^{p}n + {}^{v}n, \qquad \textbf{[1]}$$

where ^{p}n is nearly the same as proton in number and distribution, and ^{v}n = 2(2^2, 2^3, 2^4) are valency neutron holes in A, B and C steps of nuclei, respectively (Fig. 2*A*), e.g. ^{132}Xe = 54 + 54 + 2(2^2+2^3) in Table 1. As shown in Fig. 2*A*, a natural element (nucleus) at most comprise 40 ^{v}n derived from the 2-6 layers. In addition, in a nucleus ^{v}n approximates to α in number, e.g., ^{132}Xe = 24(^{v}n+α) + $_{6}$12, where $_{6}$12 is its core in $_{Z}A$ (*Z* = 6, *A* = 12, its structure is very different from a ^{12}C); the $_{6}$12 might be replaced by a $_{6}$18 in ^{222}Rn (Table 1), even in ^{302}118 (*Z* = 118, fig. S118*B*), a 6n-6p-6n sandwich core.

Table 1 shows an interesting phenomenon that grown masses are an odd number in most cases, in particular, 1, 3, 1, 3, 1, 3 and 5 in the 3rd period that when grow from odd to even *Z*, only fill 1 ^{l}p (^{23}Na^{100}→^{24}Mg^{1010}) or with 4 ^{v}n (^{35}Cl^{4443}→^{40}Ar$_{v\text{-}4}$^{4444}), but 1 ^{l}p is often accompanied by 2 ^{p}n (^{28}Si^{2222}→^{31}P^{4232}) from even to odd *Z*. Commonly, isotopic mass change for light nuclei was ^{p}n as ^{16,17,18}O in Fig. 2*B*. For mid-heavy nuclei, e.g., ^{108}Sn$_{v\text{-}8}$^{2222} (10.5 min) and ^{124}Sn$_{v\text{-}20}$^{3333} (5.94%), both the ^{p}n and ^{v}n were varied (Table 2).

In some cases this primary neutron fit is alternative. For example, a ^{36}S (0.014%) is ^{36}S$_{v\text{-}4}$^{4242} (fig. S16*D*) or ^{36}S$_{v\text{-}2}$^{4343} that how to balance ^{p}n and ^{v}n, and 20 ^{v}n of ^{127}I is v-0,4,8,8 (fig. S53) or v-4,4,8,4 (Table 1) in the 2-5 layers. Perhaps, in a nucleus neutron different distributions are corresponding to that nuclear isomers (18) (marked m1, m2, m3…), while its proton frame is unconcerned; e.g., ^{79}Br$_{v\text{-}4,4}$ (50.69%) and ^{79m}Br$_{v\text{-}0,0,8}$ (4.86 s), its inner 8 ^{v}n would be excited to outer (figs. S35*A*-*B*), or other distributions in the 2-4 layers. For nuclei, however, figs. S3*A*-18*C* indicate that: the higher is the abundance (half-life), the more concise is the structure, such as ^{12}C^{2222} (98.89%), ^{13}C^{3222} (1.11%), ^{14}C^{3232} and ^{28}Si^{2222} (92.2%), ^{29}Si^{3222} (4.7%), ^{30}Si^{3232} (3.1%).

Table 2. A tentative arrangements of $^{100-132}$Sn.

Commonly, in these 32 neutrons (132 - 100), ^{v}n ~ 20, ^{p}n ~ 8, and 4 n in the 6th layer is neutron skin (halo), meaning that Sn isotopes might only grow ^{v}n from $A >$ ^{120}Sn. All of valency neutrons in the 2-6 layers is compiled in a column.

Sn isotope	core+middle	valency neutron	axial configuration		abundance% / half-life
100	76	0, 4	b-4444	a-1111	1.1 s
108	-	0, 4, 4	-	2222	10.5 min
109	-	0, 4, 4	-	3222	18.0 min
110	-	0, 4, 4	-	3232	4.0 h
111	-	0, 4, 4	-	3332	35.3 min
112	-	0, 4, 4	-	3333	0.96
113	-	0, 4, 8	-	3222	115.2 d
114	-	0, 4, 8	-	3232	0.66
115	-	0, 4, 8	-	3332	0.35
116	-	0, 4, 8	-	3333	14.3
117	-	4, 4, 8	-	3222	7.61
118	-	4, 4, 8	-	3232	24.03
119	-	4, 4, 8	-	3332	8.58
120	-	4, 4, 8	-	3333	32.85
121	-	4, 4, 8, 1	-	-	~50 yr
122	-	4, 4, 8, 2	-	-	4.72
123	-	4, 4, 8, 3	-	-	129 d
124	-	4, 4, 8, 4	-	-	5.94
125	-	4, 4, 8, 5	-	-	9.65 d
126	-	4, 4, 8, 6	-	-	2.3×10^{5} yr
127	-	4, 4, 8, 7	-	-	2.12 h
128	-	4, 4, 8, 8	-	-	60.0 min
129	-	4, 4, 8, 8, 1	-	-	7.5 min
130	-	4, 4, 8, 8, 2	-	-	3.72 min
131	-	4, 4, 8, 8, 3	-	-	61 s
132	-	4, 4, 8, 8, 4	-	-	40.6 s

Unstable nuclei. Away from the beta stable line, ^{3}He was estimated to generate in skin of neutron-deficient light nuclei, e.g. ^{19}Ne$_{c\text{-}2+2}^{4443}$ (17.4 s) and ^{17}Ne$_{c\text{-}2+2}^{\underline{4333}}$ (0.108 s). Furthermore, a heavy nucleus lack of neutrons, ^{v}n, to bind its vertical A-5α, B-3α and C-1α clusters may more easily cause decay (emission) (19, 20), corresponding to the fact that α-decay only happen in neutron-deficient side in a range Z ~ 62-82 (in mid nuclei almost never) that begin to grow C-1α clusters, where also likely is a point of fission α-particle (Fig. 2*A*). To some extent, both α and cluster decay seem to result from the 16 α-clusters cleft into 15:1 similar to nuclear fission that only cleft ratios are different (Table 3).

In neutron-rich nuclei, neutron halo might often perch on top of axial extended lines; e.g., a structure of ^{31}F-$^{2}1^{2}$,$_{4}2^{a\text{-}4443}$,$3^{a\text{-}0000,b\text{-}0000}$ was 4 ^{v}n with other 8 n (neutron halo) to cage ^{19}F-$^{2}1^{2}$,$2^{a\text{-}4443}$ (figs. S9*A-B*). In addition, a neutron skin (halo) may happen in a stable nucleus; e.g., ^{136}Xe-$^{6}1^{6}$,$^{8}_{4}2^{8}$,$^{8}_{4}3^{8}$,$^{16}_{8}4^{16}$,$^{16}_{8}5^{16}$,$6^{b\text{-}0000}$ (8.9%), this 4 n ($6^{b\text{-}0000}$) skin will float on ^{132}Xe, because its ^{p}n and ^{v}n shells are closed.

Note that, unexpectedly, all of Z , ^{p}n and ^{v}n three shells closed ($A = 2Z + {}^{v}$n, ideal nucleus) shows not a most stable structure from two abundance (half-life) lines of ideal nuclei and their maximal abundant isotopes (Table 1) intersecting at ^{132}Xe$_{v\text{-}4,4,8,8}$ (26.89%), i.e., for ideal nuclei, the ^{v}n too many in ^{24}Ne$_{v\text{-}4}$ (3.38 min), ^{44}Ar$_{v\text{-}4,4}$ (11.87 min) and ^{88}Kr$_{v\text{-}4,4,8}$ (2.84 h), but too few in ^{212}Rn$_{v\text{-}4,4,8,8,16}$ (23.9 min). Nevertheless, here was unable to find a better way to fit pair and valency neutrons with the line of beta stability. In the followings, it seems that released neutrons may generally come from ^{v}n, not ^{p}n in fission.

Fission configuration

As fission can direct reflect details of a nuclear structure, there is an attempt to depict it to test this nucleon distributions; at this stage that fission configuration has not been very clear a brief depiction may be more effective. Generally, nuclei can occur asymmetric and symmetric fission (21-23, 28-35). Asymmetric fission shows peaking to Z = (86+102) / 2 = 94 in thermal neutron (n,f) and spontaneous (sf) fission, where 86 and 102 are A and C closed shells, implying that it may only occur within the two shells. Its process is possible that: when a neutron land on a nuclear skin and induce the skin particles to glide, more or less, to the one side, or from side to side repeatedly, then the nucleus would be cleft, likely in that when its shape is just unfolded and thus its cleft place is a line, not a point, somewhat similar to a crystal cleft. If increase excitation energy, the particles on the skin has insufficient time to glide and the core, a relatively firm six neutron center, might be broken up, thus a symmetric fission will happen. Accordingly, the core, middle and skin of a folding nucleus may play different parts in fission.

Table 3. Some fission types and paths of ^{236}U.

Fission type (different divide of core $_6$12 nucleons) was mainly classified into: 1/2, $_3$6:$_3$6; 1/4, $_3$3:$_3$9; 0, 0:$_6$12. The $^{\nu}$n number error is about $\pm$3 in mass division, which could be related to isotopic products. Skin nucleons and valency neutrons in the scission lines have not been allotted to cluster decay.

fission type and path	cleft ratio of 16 α-clusters	*Z*-*A* distribution A_L	A_H
1-1/2-9	$2^a2^b4^c : 2^a2^b4^c$ (8 : 8)	^{118}Pd	^{118}Pd
2-1/2-9	$2^a2^b3^c : 2^a2^b5^c$ (7 : 9)	^{111}Tc	^{125}In
3-1/2-9	$2^a1^b3^c : 2^a3^b5^c$ (6 : 10)	^{95}Rb	^{141}Cs
4-1/2-9	$2^a1^b2^c : 2^a3^b6^c$ (5 : 11)	^{88}Se	^{148}Ce
1-1/4-8	$1^a2^b4^c : 3^a2^b4^c$ (7 : 9)	^{94}Kr	^{142}Ba
2-1/4-8	$1^a2^b3^c : 3^a2^b5^c$ (6 : 10)	^{85}As	^{151}Pr
3-1/4-8	$1^a1^b3^c : 3^a3^b5^c$ (5 : 11)	^{69}Co	^{167}Tb
4-1/4-8	$1^a1^b2^c : 3^a3^b6^c$ (4 : 12)	^{60}Cr	^{176}Er
1-0-9	$2^a2^b4^c : 2^a2^b4^c$ (8 : 8)	^{112}Tc	^{124}In
2-0-9	$2^a2^b3^c : 2^a2^b5^c$ (7 : 9)	^{105}Zr	^{131}Te
3-0-9	$2^a1^b3^c : 2^a3^b5^c$ (6 : 10)	^{89}Se	^{147}Ce
4-0-9	$2^a1^b2^c : 2^a3^b6^c$ (5 : 11)	^{82}Ga	^{154}Pm
Cluster decay			
1-0-2	1^c : $4^a4^b7^c$ (1 : 15)	^{4}He	^{323}Th
2-0-3	1^b : $4^a3^b8^c$ (1 : 15)	^{12}C	^{224}Rn
4-0-5	1^a : $3^a4^b8^c$ (1 : 15)	^{20}Ne	^{216}Pb

Fragment structures. On the whole, fragment charge and mass is a statistical distribution. In Fig. 2*A* it appears to come from 16 α-clusters of a nucleus cleft into different ratios (colonies, Table 3), in which asymmetric fission is a double peak yield curve (21-23) that a contribution of skin particle glide might be involved. As a shift ratio of ^{m}s is a random distribution at present, while ^{m}c (^{212}Rn^{4444}, fig. S86*A*, ^{208}Pb^{3333}+4^{l}p, Fig. 2*A*) has several fixed divisions, a fission system ($_{Z}A >$ ^{212}Rn) is resolved: X = ^{m}c + ^{m}s. Thus, a fragment often is a mixture of ^{m}c and ^{m}s. For example, in 1-1/4-8 fission of ^{235}U+n, a structure of ^{235}U being $^{6}1^{6}$,$^{8}4^{2}2^{8}$,$^{8}4^{3}3^{8}$,$^{16}_{8}4^{16}$,$^{16}_{8}5^{16}$,$^{32}_{16}6^{32}$,7$^{a-0000,b-0000,c-2222}$-^{2220}, the ^{m}c is lined off:

^{212}Rn $_{1\text{-}1/4\text{-}8}$ → $_{53}129 + _{33}83$, **[2]**

where subscript is fission path that its image is somewhat analogous to a tetrahedron cutting off an angle (1 A axis, 3:1, $3^a2^b4^c$:$1^a2^b4^c$) nearby center, and the ^{m}s falls into

a-000,b-00,c-222$\underline{2}$ + a-0,b-00,c-222$\underline{2}$ = $_3$13 + $_3$11, **[3]**

a total of 24 nucleons on the skin including a thermal neutron; then add Eq. 3 to Eq. 2,

^{235}U+n $_{1\text{-}1/4\text{-}8}$ → ($_{53}$129+$_3$13) + ($_{33}$83+$_3$11) = ^{142}Ba + ^{94}Kr, **[4]**

^{235}U+n $_{1\text{-}1/4\text{-}8}$ → $_{53}$129 + ($_{33}$83+$_6$24) = ^{129}I + ^{107}Y, **[5]**

^{235}U+n $_{1\text{-}1/4\text{-}8}$ → ($_{53}$129+$_6$24) + $_{33}$83 = ^{153}Pr + ^{83}As, **[6]**

that is, when the $_3$13 glide into 1-8 sector [5] or the $_3$11 into 8-1 sector [6], they are ^{107}Y (94+13) or ^{153}Pr (142+11), suggesting that a fragment peak yield (28-31) may be partly contributed from the $_3$13 and $_3$11 glide. In Eq. 4 the ^{m}s has not glided that two fragment peak yields are near 6%.

The valley is a symmetric fission:
^{235}U+n $_{1\text{-}1/2\text{-}9}$ → $_{46}$118 + $_{46}$118, **[7]**
near 0.1% yield.

Fragment mass difference. Between two fragments, a mass difference can be setting up by a single C, B or A axis (Table 3). To an A axis, it is, e.g.,
^{235}U+n $_{1\text{-}1/2\text{-}8}$ → ($_{53}$126+$_{3}$13) + ($_{33}$86+$_{3}$11) = ^{139}Ba + ^{97}Kr = ($_{46}$118+$_{10}$21) + ($_{46}$118 - $_{10}$21), **[8]**
where $_{10}$21 = $_{10}$20 + 1, a cluster of 5 α (A3 axis) plus 1 n at A3-7 position, when the scission line sweep anticlockwise from 1-1/2-9 [7] to 1-1/2-8.

Fragment vanishing points. Fragment yields, including of A_H, A_L (22), neutron (24, 25, 36) and α-particle (21), show to vanish in the same two points at leftmost sides of double mass peaks, ~ 130 and ~ 80, which both suggest to come from an α-cluster colony where its 2 edges are enclosed by 2 A long axes, i.e., $3^a2^b4^c$ (A_H, e.g. 8-1 sector) and $2^a1^b2^c$ (A_L, e.g. 4-9 sector) α-cluster colonies. Take neutron yields for example, in
^{252}Cf $_{1\text{-}1/4\text{-}8}$ → $_{53}$129 + ($_{33}$83+$_{12}$40) = $_{53}$129 + $_{45}$123, **[9]**
where $_{53}$129 is a minimal $3^a2^b4^c$ colony, and $_{45}$123 is a complementary colony ($1^a2^b4^c$) to yield maximal neutrons (~3) (24), suggesting that maximal neutron yield is from a sector of 2 C axis edges. In ^{254}Fm (sf) that both ^{252}Cf and ^{254}Fm neutron shells may be ^{p}n-114+^{v}n-40 shows a similar result of neutron yield: minimum at 129-130 of A_H and maximum at 123-124 of A_L (36). In 4-0-9 fission, there is
^{252}Cf $_{4\text{-}0\text{-}9}$ → ($_{56}$142+$_{9}$28) + ($_{30}$70+$_{3}$12) = ^{170}Tb + ^{82}As, **[10]**
which is an extreme event that $2^a1^b2^c$+$_{3}$12 (^{82}As) has not held any ^{v}n in the scission line. In addition, it seems that a neutron deficient fragment is also nearby an enclosed $3^a2^b4^c$ or $2^a1^b2^c$ colony. For instance, in ^{238}U+^{12}C (35), a $^{73}_{33}$As likely come from $_{30}$70+$_{3}$3 in 4-1/4-9 fission, where $_{30}$70 = 5α×2+3α+1α×2+10^{v}n, a minimal $2^a1^b2^c$ colony, and $_{3}$3 is from core. For ^{72}As and ^{69}Zn in ^{238}U+p (37), they might come from other ways, such as a $1^a2^b2^c$ colony, because the 10 ^{v}n normally cannot be released inside a minimal $2^a1^b2^c$ colony ($^{70}_{30}$Zn) (35), unless one of them has become a delayed neutron (38), different from prompt neutrons (25) which might come from N1-6 and N8-6 that are ^{v}n not ^{p}n in 1-1/4-8 fission (Fig. 2*A*), when the fragment was reconstituted to turn into a daughter nucleus.

Skin particle glide. Comparing Eq. 5 and Eq. 6 suggests that the ^{m}s prefer to glide upon top of A_L ($3^a2^b4^c$:$1^a2^b4^c$+ ^{m}s), for the yield of Eq. 5 is usually higher than Eq. 6. This view is also illustrated by that A_H masses are nearly constant, while A_L masses increase in ^{229}Th, ^{233,235}U, ^{239}Pu, ^{245}Cm, ^{249}Cf and ^{254}Es (n,f) (22). However, particles at skin may glide limited in the two closed shells that transition from asymmetry to symmetry is in two sides of Z 94±6 ($_{88}$Ra-$_{100}$Fm) (39), implying that its mass number is neither too many, nor too few. For example, in the light side of Z 94±6 there is ^{226}Ra (^{3}He, df) that simultaneously reveal asymmetric and symmetric fission (40). In the heavy side of Z 94±6, transition is in Fm isotopes (36, 39, 41-43), which from $^{254}_{100+114+40}$Fm$^{a\text{-}0000,b\text{-}\underline{2222},c\text{-}4443\text{-}4443}$ (sf, asymmetric) to $^{258}_{100+118+40}$Fm$^{a\text{-}\underline{2222},b\text{-}\underline{2222},c\text{-}4443\text{-}4443}$ (^{257}Fm+n, symmetric), the a-0000 was replaced by the a-2222 at the top of 4 A axes (see superscript and subscript). This is likely that the closed ^{p}n-118 shell (see also fig. S100) fence against the skin particles to glide and drive a ^{258}Fm bisected. In the case of $^{252}_{102+110+40}$No$^{a\text{-}0000,b\text{-}0000,c\text{-}4444\text{-}4444}$, though its Z-102 shell is closed (see also fig. S102), it is an asymmetric fission (44), possible that it lack 8 ^{p}n than ^{258}Fm in the skin to resist the ^{m}s glide.

Possible to result in even-Z fragment that its energy release is greater than odd (fine structure of fragment masses, interval A ~ 5, ^{v}n+α) (28-31), part of skin particles might be fused in glide, since in ^{235}U (n,f), its skin having no an inherent α-particle in ground state, has occurring polar α-particle emission, about 0° or 180° with respect to the fission axis (45-47); further, it is over 3 times for A_L to A_H flight directions (46), which is in favor of the ^{m}s to glide upon A_L also. In order to clarify whether polar emission come from the ^{m}s glide, if possible, could try to detect that symmetric fission; e.g. ^{208}Pb (Fig. 2*A*) or ^{257}Fm (n,f), their ^{m}s are almost unable to glide and estimate that polar emission is less than ^{235}U (n,f).

Ternary fission, α and cluster decay. Binary fission in Fig. 2*A* could draw a line from one side through the core to the opposite side. When draw three lines, e.g., 1-c (from N1-6 to core), 2-c and 9-c. it is a ternary 1-2-9 fission. Usually, 1-2 sector (one of 8 C axes) is a place of light charged particle (LCP) emission (21, 26, 27, 48, 49) and can partition it into three points: C1-7 (p, d, t, α), C1-6 (α) and C1-6+C1-7 (^{7,8,9}Li, ^{9,10}Be). Among them most probable emission is α and its angle to differ from polar emission is perpendicular to the fission axis, nearly 90±22.5° to A_H and A_L, respectively, where 22.5° = 360°/16. Since a fission nucleus is almost impossibly complete unfolded, its α emitting angle is within 67.5°-112.5°, which is in good agreement with results reported (26, 27) that is difficult to explain up to now, to the author's knowledge. In addition, it is possible that LCP, just in the two ends of a scission line, could serve as a probe to identify axial configurations on the condition that the ^{m}s has not glided or in glide $_{Z}A$ of some LCP have not varied. LCP emission probabilities in per 10^3 sf of ^{252}Cf$^{a\text{-}0000,b\text{-}\underline{2222},c\text{-}4343\text{-}4343}$ are: α-3.3, t-0.2, d-0.02 and p-0.06, respectively (48), slightly less than ideal that its axial configuration has 4 α and 4 t, no d and p.

If the track varied from 1-2-9 to 1-4-8 randomly, it is a three large fragment fission (50, 51), in which ^{235}U (n,f), three sectors are about 1-4 (^{35}Mg), 4-8 (^{56}Sc) and 8-1 (^{145}Pr). It thus suggests that lighter fragments, including α and cluster decay, may come from a different combination of A, B and C axes, e.g., 1^{c}, A ~ 10, LCP; $1^{b}2^{c}$, A ~ 30, ^{28}Mg (51); $1^{a}1^{b}1^{c}$, A ~ 50, ^{47}Ca, ^{48}Sc (37). From here, it is tempting to expect that a nucleus might deeply be fragmented into four large fragments; e.g., in a quaternary 1-3-9-14 fission of ^{235}U+n, four sectors are 1-3 (^{25}F), 3-9 (^{93}Rb), 9-14 (^{69}Co) and 14-1 (^{49}K). However, four coincident fragment angular, energy and mass as a function of excitation energy in a quaternary fission would shed interesting light upon that whether a nuclear shape is from folded (tetrahedral 4 A axes) to unfolded (plane 4 A axes) in fission.

Discussion

In this paper, it has described that folding nuclei can grow vertical 16 α-clusters bound with valency neutrons to stand the core. In fission, some of ^{v}n in a scission line will convert into unbound neutrons and lead to the 16 α-clusters of different length cleft, like a molecular bond broken, into symmetric 8:8, or asymmetric 9:7 (Fig. 2*A*) that its a pair fragment mass difference is about 5 α × 2 = $_{20}$40 (±1 A axis, 2 clusters of 5 α), which is well consistent with data obtained (21-23), for a typical example, ^{235}U+n→^{137}Ba+^{97}Kr+2n.

To explain why two coincident fragments have a characteristic mass difference is a central problem in nuclear fission testing nuclear models. Sometimes, a heavy fragment was explained near *Z*-50, *N*-82 doubly magic shells (41) and a light fragment near *N*-50 shell (21), which might be less straightforward than this explanation that the fragment mass difference results from ±1 A axis. However, It seems that there has no a clear distinction between proton and neutron shells. Likely, their shells are the same only in magic number 2 (^{4}He), 8 (^{16}O) and 20 (^{40}Ca) (Table 1); for the 28, 50 and 82, it is to differ because of valence neutron emergence, suggesting that proton shells are constant, whereas neutron shells are not in a number. For example, *Z*-50 shell is all along fixed, when isotope mass increasing from $^{100}{}_{50+46+4}$Sn to $^{132}{}_{50+54+28}$Sn (Table 2), while *N*-50 shell has largely been changed that the ^{v}n are gradually turned into the ^{p}n to pair increased ^{l}p, when isotone charge increasing from $^{82}{}_{32+36+14}$Ge to $^{100}{}_{50+46+4}$Sn. However, it is likely different that *N*-50 shell in ^{88}Sr (^{84}Kr+a-1010) from ^{89}Y (^{84}Kr+b-11$\underline{2}$), *N*-82 shell in ^{138}Ba from ^{139}La, ^{140}Ce, ^{141}Pr and ^{142}Nd (Table 1). For that *N*-126 shell, in Fig. 2*A* shows to derive from ^{p}n-86+^{v}n-40, a frame to grow $^{208}{}_{82+86+40}$Pb^{3333}, ^{209}Bi^{4333}, ^{210}Po^{4343}, ^{211}At^{4443} and $^{212}{}_{86+86+40}$Rn^{4444}. Though only *Z*-2, *N*-2, *Z*-28 and *N*-126 shells are closed here, magic nuclei are encouragingly displayed a definite images (Figs. 2*A*-*B*), and, it is undeniable that all the magic nuclei together with their neighbor nuclei able to grow is so smooth in Table 1, which would be helpful to account for magic number phenomena in future.

On the other hand, it is possible that a nucleus might emerge different structures in ground and excited states. For example, a ^{16}O in ground state is ^{16}O$_{c\text{-}2+2}{}^{4242}$ and in excited state is 4 α-structure that skin 2 d of ^{16}O$_{c\text{-}2+2}{}^{4242}$ were combined 1 α; otherwise in ground state how a 4 α-structure of ^{16}O can carry two hydrogen atoms to build a water molecule? Whereas a ^{1}H$_2{}^{16}$O M-N structure

will have understood at a glance in Fig. 2*B*, suggesting that the action of a nucleus in a molecule might have to take into account (52). However, a compelling relation between light nuclei and simple molecules may has been carried out in this work, which is an integrative result of Lewis dot structure (3) (Table 1 and figs. S119-125) and alpha-particle model (9) plus valency neutrons to some extent. Moreover, the scope of atoms was broadened to proton distributions in addition to electron distributions, though not to incorporate them. As the proton is predominant in an atom in a sense, the element properties may essentially result from the proton, *Z*, the atomic number, which is shown to occupy constant spatial positions not only in nuclei, but also in molecules as well (Fig. 2*B*), implying that the periodic law interpreted by proton might be less complicated, that is, the proton arrangements in nuclei are likely corresponding to the element arrangements in the periodic table (Figs. 1*A-C*).

Accordingly, the periodic law seems to dominate structures of not only molecules and atoms, but nuclei. Further, this folding nuclear structure appears to be feasible in depicted typical fission phenomena. Namely, a nuclear fission is likely that its 16 α-clusters are cleft into different ratios from 15:1 (1^c, α decay; 1^b or 1^a, cluster decay, essentially similar to three large fragments in a fission) to 8:8 that a most probable ratio is 9:7 ($3^a2^b4^c$:$1^a2^b4^c$) and its charge and mass difference is about ${}_zA \geqslant {}_{20}40$ in two coincident fragments, released prompt neutrons are only valency neutrons from a scission line (Fig. 2*A*), α-particle angle within $90 \pm 22.5^\circ$ to its fission axis is emitting from one of C family 8 α-particles, and, all fragment, neutron and α-particle yields suggests to vanish in the same two points: $3^a2^b4^c$ ($A_H \sim 130$) and $2^a1^b2^c$ ($A_L \sim 80$) α-cluster colonies (21-27). Taken together, however, there is a possibility that the periodic table form is rooting in nuclei that can only grow 1 α-particle in the 1st layer (core) intensified by 4^lp of ${}_{27}$Co, ${}_{28}$Ni, ${}_{45}$Rh and ${}_{46}$Pd, and then grow 2^3, 2^4 and 2^5 α-particles together with nearly same number valency neutrons in the 2-3, 4-5 and 6-7 layers, respectively (Fig. 2*A*), which is in general agreement with the line of beta stability. Consequently, the atomic number of the 1-7 periods is derived from Z $118 = 2(1+2^3+2^4+2^5) + 4$ that noble nuclei are able to demonstrate perfect nucleon distributions (Table 1) in three dimensions. Furthermore, the number of the elements [$2(2^3+2^4+2^5)$ besides groups 9-10B] and valency neutrons ($2^3+2^4+2^5$) in the A, B and C steps being a square relation therefore indicates that an element nucleus unusually is a two dimensional structure in a nuclear phase, a folding nucleon plate; so that gives rise to it, a crude nucleon aspect was suggested from macrocosm. However, though here is an empirical distribution of nucleons, it provides a promising primary way that may be beneficial to further clarify and/or integrate nuclear, atomic and molecular structures.

Acknowledgments

This work was partly supported by Changzhou Bureau of science and technology, China. The author thanks Mr. Benlin Liu for an appreciation.

Supporting figs. S1-125 (35 MB)

References

1. Thomson JJ (1897) Cathode rays. *Phil. Mag*. **44**, 293.
2. Bohr N (1913) On the constitution of atoms and molecules. *Phil. Mag*. **26**, 476-502.
3. Lewis GN (1916) The atom and the molecule. *J. Am. Chem. Soc*. **38**, 762-785.
4. Langmuir I (1919) The arrangement of electrons in atoms and molecules. *J. Am. Chem. Soc*. **41**, 868-934.

5. Moseley HGJ (1913) The high frequency spectra of the elements. *Phil. Mag*. **26**, 1024.
6. Moseley HGJ (1914) Atomic models and x-ray spectra. *Nature* **92**, 554-554.
7. Rutherford E (1911) The scattering of α and β particles by matter and the structure of the atom. *Phil. Mag*. **6**, 21.
8. Chadwick J (1932) Possible existence of a neutron. *Nature* **129**, 312.
9. Hafstod LR, Teller E (1938) The alpha-particle model of the nucleus. *Phys. Rev*. **54**, 681.
10. Meitner L, Frisch OR (1939) Disintegration of uranium by neutrons: a new type of nuclear reaction. *Nature* **143**, 239.
11. Bohr N, Wheeler JA (1939) Phys. Rev. **56**, 426.
12. Haxel O, Jensen JHK, Suess HE (1949) On the "magic numbers" in nuclear structure. *Phys. Rev*. **75**, 1766.
13. Hahn O, Strassmann F (1939) *Naturwiss*. **27**, 89.
14. Friedlander G, Kennedy JW, Macias ES, Miller JM (1981) *Nuclear and Radiochemistry* (John Wiley & Sons, New York), p. 27.
15. Geiger H, Marsden E (1909) On a diffuse reflection of the α-particles. *Proc. Roy. Soc*. A **82**, 495-500.
16. Meyer JL, redrawn by Bayley T (1882) Phil. Mag. **13**, 26-37.
17. Bohr A, Mottelson BR (1969) *Nuclear Structure* (Benjamin, New York), vol. **1**.
18. Hahn O (1921) *Naturwiss*. **9**, 84.
19. Rose HJ, Jones GA (1984) A new kind of natural radioactivity, *Nature* **307,** 245-247. doi: 10.1038/307245a0.
20. Andreyev AN et al. (2013) Signatures of the Z = 82 shell closure in α-decay process. *Phys. Rev. Lett*. **110**, 242502. doi: 10.1103/PhysRevLett.110.242502.
21. Schmitt HW, Neiler JH, Walter FJ, Chetham-Strode A (1962) Mass distribution and kinetics of ^{235}U thermal-neutron-induced three-particle fission. *Phys. Rev. Lett*. **9**, 427-429.
22. Unik JP et al. (1973) Fragment mass and kinetic energy distributions for fissioning systems ranging from 230 to 256. *Proc. IAEA Symp. Phys. Chem. Fission*, **2**, 19-46.
23. Dickens JK, McConnell JW (1986) Yields of fission products produces by thermal-neutron fission of ^{243}Cm. *Phys. Rev*. C **34**, 722-725.
24. Bowman HR, Milton JCD, Thompson SG, Swiatecki WJ (1963) Further studies of the prompt neutrons from the spontaneous of ^{252}Cf. *Phys. Rev*. **129**, 2133-2147.
25. Terrell J (1965) Prompt neutrons from fission. *Proc. IAEA Symp. Phys. Chem. Fission*, **2**, 3-24.
26. Fraenkel Z, Thompsom SG (1964) Properties of the alpha particles emitted in the spontaneous of ^{252}Cf. *Phys. Rev. Lett*. **13**, 438-441.
27. Fluss MJ, Kaufman SB, Steinberg EP, Wilkins BD (1973) Angular distribution in the spontaneous fission of ^{252}Cf. *Phys. Rev*. C **7**, 353-364.
28. Thomas TD, Vandenbosch R (1964) Correlation of fission-fragment kinetic-energy fine structure with a semiempirical surface. *Phys. Rev*. **133**, B976-982.
29. Reisdorf WN, Unik JP, Glendenin LE (1973) Correlation between fragment mass-distribution fine structure, charge distribution and nuclear structure for thermal-neutron-induced fission of ^{233}U and ^{235}U. *Nucl. Phys*. A**205**, 348-362.
30. Schmitt HW, Neiler JH, Walter FJ (1966) Fragment energy correlation measurements for ^{252}Cf spontaneous fission and ^{235}U thermal-neutron fission. *Phys. Rev*. **141**, 1146-1160.

31. Neiler JH, Walter FJ, Schmitt HW (1966) Fission-fragment energy-correlation measurements for the thermal-neutron fission of ^{239}Pu and ^{241}Pu. *Phys. Rev*. **149**, 894-905.

32. Plasil F, Ferguson RL, Pleasonton F (1973) Neon-induced fission of silver. *Proc. IAEA Symp. Phys. Chem. Fission*, **2**, 319-333.

33. Wilkins BD et al. (1984) Mass and kinetic energy distribution in near-barrier fission of ^{182}W. *Phys. Rev*. C **30**, 1228-1232.

34. Hulet EK et al. (1986) Bimodal symmetric fission observed in the heaviest elements. *Phys. Rev. Lett*. **56**, 313-316.

35. Delaune O et al. (2013) Isotopic yields distributions of transfer- and fution-induced fission from ^{228}U + ^{12}C reactions in inverse kinematics. *Phys. Rev*. C **88**, 024605. doi: 10.1103/PhysRevC.88.024605.

36. Gindler JE, Flynn KF, Glendenin LE, Sjoblom RK (1977) Distribution of mass, kinetic energy and neutron yield in the spontaneous of ^{254}Fm. *Phys. Rev*. C **16**, 1483-1491.

37. Klingensmith DL, Porile NT (1988) Fragment emission in the interaction of ^{238}U with 400 Gev protons. *Phys. Rev*. C **38**, 818-831.

38. Amiel S (1969) Delayed neutrons in fission. *Proc. IAEA Symp. Phys. Chem. Fission*, 569-590.

39. Ragaini RC, Hulet EK, Lougheed RW, Wild J (1974) Symmetric fission in the neutron-induced fission of ^{255}Fm. Phys. Rev. C **9**, 399-406.

40. Konecny E, Specht HJ, Weber J (1973) Symmetric and asymmetric fission of Ra- and Ac-isotopes. *Proc. IAEA Symp. Phys. Chem. Fission*, **2**, 3-18.

41. Balagna JP, Ford GP, Hoffman DC, Knight JD (1971) Mass symmetry in the spontaneous fission of ^{257}Fm. *Phys. Rev. Lett*. **26**, 145-148.

42. John W, Hulet EK, Lougheed RW, Wesolowski JJ (1971) Symmetric fission in thermal-neutron-induced and spontaneous fission of ^{257}Fm. *Phys. Rev. Lett*. **27**, 45-48.

43. Flynn KF, Gindler JE, Glendenin LE (1975) Distribution of mass in thermal-neutron-induced fission of ^{257}Fm. *Phys. Rev*. C **12**, 1478-1482.

44. Bemis CE et al. (1977) Fragment-mass and kinetic-energy distributions from the spontaneous fission of ^{252}No. *Phys. Rev*. C **15**, 705-712.

45. Piasecki E, Dakowski M, Krogulski T, Tys J, Chwaszczewska J (1970) Evidence of the polar emission of alpha-particles in the thermal neutron fission of ^{235}U. *Phys. Lett*. **33**B, 568-570.

46. Piasecki E, Dakowski M, Kordyasz A (1973) Recent studies on polar emission. *Proc. IAEA Symp. Phys. Chem. Fission*, **2**, 383-388.

47. Piasecki E, Nowicki L (1979) Polar emission in fission. *Proc. IAEA Symp. Phys. Chem. Fission*, **2**, 193-221.

48. Wild JK et al. (1985) Light-charged-particle emission in the spontaneous fission of ^{250}Cf, ^{256}Fm and ^{257}Fm. *Phys. Rev*. C **32**, 488-495.

49. Wagemans C, D'hondt P, Schillebeeckx P, Brissot R (1986) Triton and alpha emission in the thermal-induced ternary fission of ^{233}U, ^{235}U, ^{239}Pu and ^{241}Pu. *Phys. Rev*. C **33**, 943-953.

50. Muga ML, Rice CR, Sedlacek A (1967) Ternary fission of heavy nuclei. *Phys. Rev. Lett*. **18**, 404-408.

51. Iyer RH, Cobble JW (1966) Evidence of ternary fission at lower energies. *Phys. Rev. Lett*. **17**, 541-545.

52. Yixing C et al. (2016) Electrolytes induce long-range orientational order and free energy changes in the H-bond network of bulk water. *Science Advances*. Vol. **2**, no. 4, e1501891. doi: 10.1126/sciadv.1501891.